Physics Letters B 670 (2008) 37–40

Contents lists available at ScienceDirect

Physics Letters B

www.elsevier.com/locate/physletb

Explaining the DAMA signal with WIMPless dark matter

Jonathan L. Feng, Jason Kumar *, Louis E. Strigari

Department of Physics and Astronomy, University of California, Irvine, CA 92697, USA

ARTICLE INFO

Article history:
Received 21 September 2008
Accepted 17 October 2008
Available online 29 October 2008
Editor: S. Dodelson

PACS:
95.35.+d
04.65.+e
12.60.Jv

ABSTRACT

WIMPless dark matter provides a framework in which dark matter particles with a wide range of masses naturally have the correct thermal relic density. We show that WIMPless dark matter with mass around 2–10 GeV can explain the annual modulation observed by the DAMA experiment without violating the constraints of other dark matter searches. This explanation implies distinctive and promising signals for other direct detection experiments, GLAST, and the LHC.

1. Introduction

Dark matter makes up 24% of the energy density of the Universe, but its identity is unknown. At present all incontrovertible evidence for dark matter is based on its gravitational interactions. As the requisite first step toward identifying dark matter, diverse experiments worldwide are searching for evidence for additional dark matter interactions, with several tentative hints reported so far.

By far the most significance claimed for a non-gravitational signal is the DAMA Collaboration's observation [1] of annual modulation [2] in recoil scattering off NaI(Tl) detectors deep underground at the Gran Sasso National Laboratory. When combined with previous results [3], these recent data yield an 8.2σ signal based on a total exposure of 0.82 ton-years. The observed modulation has period $T = 0.998 \pm 0.003$ years and maximum at $t = 144 \pm 8$ days, both perfectly consistent with the values $T = 1$ year and $t = 152$ days expected for dark matter, given simple astrophysical assumptions.

Experimental aspects of the DAMA result have been the topic of lively discussion, to which we have nothing to add. From a theoretical viewpoint, however, the DAMA result is also very interesting, because it has not been easy to reconcile with other experimental constraints or to explain with candidates that are motivated by considerations other than the DAMA anomaly itself. Of course, comparisons with other experiments and theory are model-dependent, requiring additional assumptions from both particle physics and astrophysics. At the same time, it is likely that a definitive discovery of dark matter will require confirmation by more than one experiment under the unifying umbrella of a plausible theoretical framework. Toward this end, we here propose a dark matter explanation that has well-motivated features and then determine other observable predictions that may be used to exclude or favor the proposed explanation.

2. DAMA regions

The DAMA signal is consistent with the scattering of dark matter particles X through elastic, spin-independent interactions. The conventional region has mass and X–nucleon cross section $(m_X, \sigma_{\rm SI}) \sim$ (20–200 GeV, 10^{-5} pb) [4]. This is now excluded, most stringently by XENON10 [5] and CDMS (Ge) [6], which require $\sigma_{\rm SI} < 10^{-7}$ pb throughout this range of m_X. Spin-dependent and other more general couplings do not remedy the situation [7]. Mirror dark matter has been proposed as a solution [8], as has inelastic scattering, where the dark matter particle is accompanied by a companion particle that is roughly ~ 100 keV heavier [9].

Gondolo and Gelmini have noted, however, that an alternative region with $(m_X, \sigma_{\rm SI}) \sim$ (1–10 GeV, 10^{-3} pb) may explain the DAMA results without violating other known bounds [10]. DAMA's relative sensitivity to this region follows from its low energy threshold and the lightness of Na nuclei. This region is extended to lower masses and cross sections by the effects of channeling [11–13] and may also be broadened if dark matter streams exist in the solar neighborhood [10], arising, for example, from the destruction of Galactic satellites [14,15]. The allowed region is constrained by null results from CRESST [16], CDMS (Si) [17], TEXONO [18] (see, however, Ref. [19]), and CoGeNT [20]. Even including all these bounds, however, there is an allowed region when channeling or streams are included, as illustrated in Fig. 1.

Unfortunately, the low mass DAMA region is very difficult to realize in standard weakly-interacting massive particle (WIMP)

* Corresponding author.
E-mail address: jkumar@hawaii.edu (J. Kumar).

0370-2693/$ – see front matter
doi:10.1016/j.physletb.2008.10.038

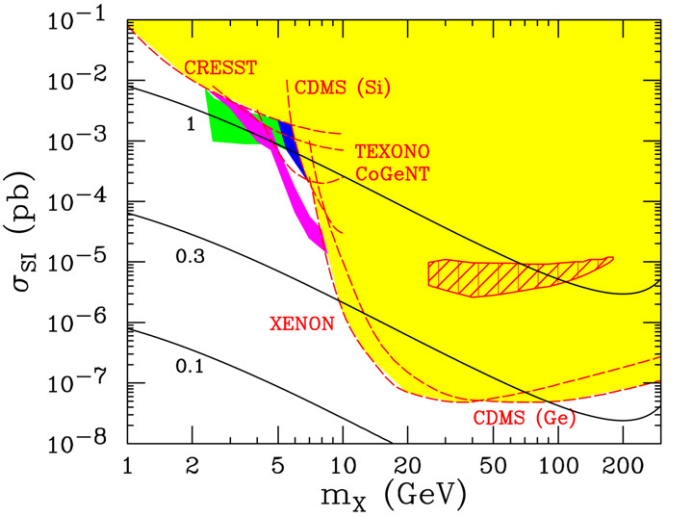

Fig. 1. Direct detection cross sections for spin-independent X–nucleon scattering as a function of dark matter mass m_X. The solid curves are the predictions for WIMPless dark matter with connector mass $m_Y = 400$ GeV and the Yukawa couplings λ_b indicated. The light yellow shaded region is excluded by the experimental results indicated (see text). The dark blue shaded region is consistent with the DAMA signal at 3σ, using 2–4 and 6–14 keVee bins; it may be extended to the medium green shaded region with the inclusion of dark matter streams and 2–6 and 6–14 keVee bins [10]. The medium-dark magenta shaded region is DAMA-favored when channeling is included (but streams are not) [12]. The cross-hatched region is the conventional DAMA-favored region [4], which is now excluded by other experiments. (For interpretation of the references to color in this figure legend, the reader is referred to the web version of this Letter.)

frameworks. In the minimal supersymmetric standard model (MSSM) with gaugino mass unification, for example, the neutralino mass is constrained to be above 46 GeV [21]. This may be evaded by relaxing gaugino mass unification. The cross section is, however, a much more robust problem. Spin-independent scattering requires a chirality flip on the quark line. In supersymmetric models with minimal field content and other well-known WIMP frameworks, σ_{SI} is thus highly suppressed by Yukawa couplings. Neutralino cross sections as high as 8×10^{-5} pb are possible and may explain the DAMA signal [22], but more typically, σ_{SI} falls short of this value by many orders of magnitude.

3. WIMPless models

WIMPless dark matter provides a framework in which dark matter candidates with a wide range of masses naturally have the correct thermal relic density [23]. In WIMPless models, the standard supersymmetric model with gauge-mediated supersymmetry breaking is supplemented by a hidden sector, consisting of particles with no standard model (SM) gauge interactions. The hidden sector contains the WIMPless dark matter particle, which has mass m_X at the hidden sector's supersymmetry breaking scale and interacts through hidden sector gauge interactions with coupling g_X. Supersymmetry breaking in a single sector is transmitted through gauge interactions to both the MSSM and the hidden sector. As a result,

$$\frac{m_X}{g_X^2} \sim \frac{m_W}{g_W^2}, \tag{1}$$

where $m_W \sim 100$ GeV–1 TeV and $g_W \simeq 0.65$ are the weak mass scale and gauge coupling. Because the thermal relic density of a stable particle is

$$\Omega \propto \frac{1}{\langle \sigma v \rangle} \sim \frac{m^2}{g^4}, \tag{2}$$

$\Omega_X \sim \Omega_W$, the thermal relic density of a typical WIMP. Since this is known to be approximately the observed dark matter density, these hidden sector particles also have approximately the observed dark matter density, preserving the key virtue of WIMPs. At the same time, WIMPless dark matter need not have weak-scale mass, and so provides a promising scenario to explain the DAMA signal in the low mass region with parameters $m_X \sim 2$–10 GeV and $g_X \sim 0.1$.

4. Direct detection

Of course, a valid DAMA explanation also requires the correct σ_{SI}. WIMPless dark matter has no SM gauge interactions, but may have non-gauge interactions with SM particles without spoiling the motivations detailed above [23,24]. In fact, intersecting brane models motivate connector particles Y, charged under both SM and hidden sector gauge groups, to mediate such interactions [25]. Consider the interactions

$$\mathcal{L} = \lambda_f X \bar{Y}_L f_L + \lambda_f X \bar{Y}_R f_R, \tag{3}$$

where X is a scalar WIMPless candidate, the connectors $Y_{L,R}$ are chiral fermions, and $f_{L,R}$ are SM fermions. These terms mediate spin-independent X-nucleus scattering via $Xq \to Y \to Xq$ with cross section

$$\sigma_{SI} = \frac{1}{4\pi} \frac{m_N^2}{(m_N + m_X)^2} \left[\sum_q \frac{\lambda_q^2}{m_Y - m_X} \left[Z B_q^p + (A - Z) B_q^n \right] \right]^2, \tag{4}$$

where we have assumed X is not its own anti-particle, and Z and A are the atomic number and mass of the target nucleus N. For the light quarks $q = u, d, s$, $B_q^{p,n} = \langle p, n | \bar{q} q | p, n \rangle \equiv m_{p,n} f_q^{p,n} / m_q$. For the heavy quarks, nucleon scattering arises through gluon couplings induced by triangle diagrams with the quarks in the loop. These diagrams can be computed simply from anomaly considerations [26], and one finds $B_q^{p,n} = (2/27) m_p f_g^{p,n} / m_q$ for $q = c, b, t$, where $f_g^{p,n} = 1 - f_u^{p,n} - f_d^{p,n} - f_s^{p,n}$. Reasonable values for the hadronic parameters are $B_u^p = B_d^n \simeq 6$, $B_d^p = B_u^n \simeq 4$, $B_s^{p,n} \simeq 1$, and $f_g^{p,n} \simeq 0.8$ [27].

The connectors Y are similar to 4th generation quarks. They get mass from both SM and hidden gauge couplings, and so we expect $m_Y \sim \max(m_W, m_X)$; given that we are interested in the DAMA signal with $m_X < m_W$, this implies $m_Y \sim m_W$. The Yukawa couplings λ_q are model-dependent. If all are $\mathcal{O}(1)$, these couplings would violate flavor bounds. We will assume that only λ_b and λ_t are significant. These are the least constrained experimentally, and it is reasonable to assume that the others are Cabbibo-suppressed. Top quark contributions to σ_{SI} are suppressed by m_t, and so with this assumption, σ_{SI} is dominated by the coupling to the b quark.

The results for σ_{SI} for X-proton scattering as a function of m_X are given in Fig. 1 for various values of λ_b. For $\lambda_b \sim 0.5$, σ_{SI} is in the required range to explain the DAMA signal. The WIMPless model therefore matches both the required mass and cross section without difficulty. Note that σ_{SI} is much larger than is typical for WIMPs. The problem of chirality flip suppression noted above is solved by introducing a heavy fermion as an intermediate state. This possibility was noted previously for scalar dark matter in another context [28]. In WIMPless models, this general solution arises naturally, with the "4th generation quarks" $Y_{L,R}$ playing the role of heavy fermions. As with any other proposal that targets the low mass DAMA-favored region, this explanation will be tested by progress in direct detection from, for example, future analyses of CDMS data and ultra-low threshold experiments [29].

5. Indirect detection

We now focus on the DAMA-favored parameter region without dark matter streams, where $m_X \gtrsim 5$ GeV. The interactions of Eq. (3) will also mediate $X\bar{X} \to b\bar{b}$ via t-channel Y exchange. These quarks will hadronize and decay into showers of photons, e^+, e^-, and neutrinos, providing interesting signals for indirect dark matter detection at a variety of experiments.

The annihilation cross section for $X\bar{X} \to b\bar{b}$ is

$$\sigma_{b\bar{b}} v = \frac{\lambda_b^4}{4\pi} \frac{m_Y^2}{(m_X^2 + m_Y^2)^2} \sqrt{1 - \frac{m_b^2}{m_X^2}}. \tag{5}$$

This depends on several unknown parameters. However, requiring that this WIMPless dark matter fit the low mass DAMA region fixes $m_X \ll m_N, m_Y$. In this limit, both $\sigma_{\rm SI}$ and $\sigma_{b\bar{b}} v$ depend on λ_b and m_Y only through the combination λ_b^2/m_Y. Requiring that $\sigma_{\rm SI}$ fit the DAMA-favored value then fixes $\sigma_{b\bar{b}} v \simeq 2 \times 10^{-25}$ cm^3 s$^{-1} \simeq 7$ pb, completely determining the predicted signal at indirect detection experiments in this model. The cross-section for WIMPless dark matter to annihilate to hidden sector particles via hidden gauge interactions is of approximately the same order of magnitude, yet the total annihilation cross-section cannot be too large if the WIMPless candidate is to be a significant dark matter component. But for WIMPless dark matter (unlike neutralinos) the precise relation between the total annihilation cross section and the relic density depends on some model-dependent factors, such as the ratio of hidden and visible sector temperatures and the number of relativistic degrees of freedom in the hidden sector [24]. For reasonable choices of these parameters, this WIMPless model can have a relic density that is 10–100% of the observed density of dark matter.

We focus now on photon detection prospects [30]. The shape of the photon spectrum is determined by the $b\bar{b}$ annihilation channel; it is given in Ref. [31], and $E^2\, d\Phi/dE$ peaks at $E \approx m_X/25$. The normalization is determined by $\sigma_{b\bar{b}} v$, the experiment's angular resolution, and the halo profile. We assume an angular resolution $\Delta\Omega = 10^{-3}$ sr and choose an NFW halo profile [32], which matches both the local density of 0.3 GeV cm^{-3} and the halo mass of $7 \times 10^{11} M_\odot$ within 100 kpc [33]. These halo parameters may vary by factors of 2 or more. This is a moderate profile, with $\rho \propto r^{-0.8}$ in the Galactic center and cuspiness parameter $\bar{J} = 4$. We note, however, that the photon spectrum normalization may be smaller, with profiles with $\rho \propto r^{-0.4}$ yielding $\bar{J} \sim 1$.

In Fig. 2 we plot the resulting γ-ray spectrum for $m_X = 6$ GeV, and $\sigma_{b\bar{b}} v = 2 \times 10^{-25}$ cm^3 s^{-1}. Also plotted is EGRET's γ-ray spectrum from the Galactic center region [34]. We see that, even for a standard halo profile, WIMPless models predict spectra that may be as large as allowed by current data. Such signals provide a promising target for the recently launched Gamma-ray Large Area Space Telescope (GLAST). As expected, the spectrum peaks near 0.2 GeV. Internal bremsstrahlung, so promising because its $E^2\, d\Phi/dE$ peaks very near m_X, is unfortunately suppressed in this case by the high mass of the final state b quarks [35]. Nevertheless, the peak in $E^2\, d\Phi/dE$ at $E \approx 0.2$ GeV provides a specific observable prediction of this model.

Although we have focused on γ-rays from the Galactic center, the large annihilation cross section may make it possible to detect γ-rays from other sources in the halo, for example from the diffuse emission away from the Galactic center or from dark matter-dominated Galactic satellites. These latter objects may provide a more robust signal given the reduced backgrounds and more well-measured dark matter distributions. For example, scaling the results of Ref. [36] to the masses and cross sections for WIMPless models, we find fluxes integrated over solid angles

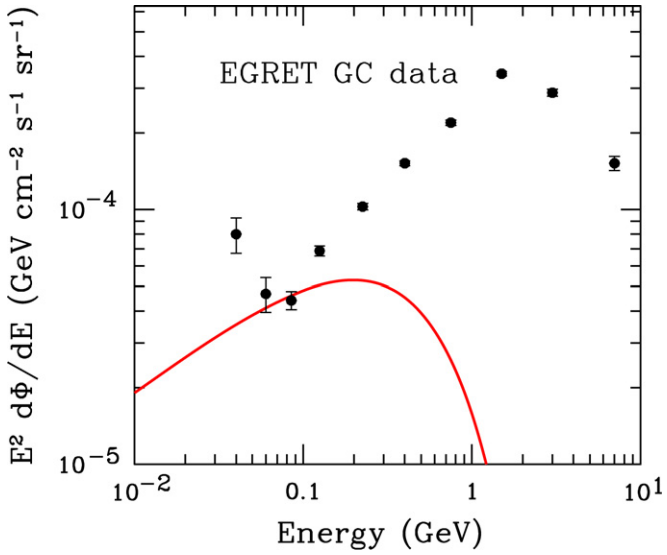

Fig. 2. Predicted γ-ray spectrum for a WIMPless model that explains DAMA with $m_X = 6$ GeV and $\sigma_{b\bar{b}} v = 2 \times 10^{-25}$ cm^3 s^{-1} and an NFW halo profile (see text). The data are EGRET's γ-ray spectrum from the Galactic center [34].

of 10^{-10}–10^{-9} cm^{-2} s^{-1} GeV^{-1} from the nearest satellites, also within reach of GLAST.

The annihilation process $X\bar{X} \to b\bar{b}$ also produces positrons [37]. For the model we consider, where $\sigma_{b\bar{b}} v \simeq 2 \times 10^{-25}$ cm^3 s^{-1}, with certain assumptions about the local dark matter density [38], the e^+ flux can be competitive with that observed by HEAT [39]. Though this signal is affected by astrophysical uncertainty in e^+ propagation, experiments like PAMELA may be sensitive to wide regions of WIMPless parameter space, providing another interesting channel for study.

6. Collider signatures

This WIMPless model also has distinctive signatures for the Large Hadron Collider (LHC). The most dramatic signatures are from production of the exotic connector quark multiplets $Y_{L,R}$. These get mass from electroweak symmetry breaking and are constrained by direct searches at the Tevatron, corrections to precision electroweak observables, and perturbativity [40]. These constraints require 260 GeV $\lesssim m_Y \lesssim$ 500 GeV. In this mass range, the process $pp \to Y\bar{Y} \to X\bar{X}b\bar{b}$ should be observable at the LHC, and the combination of this signature with typical gauge-mediation signatures, for example, long-lived sleptons, multi-lepton or prompt photon events, is distinctive. Monojet and single photon signals from $pp \to X\bar{X}(j, \gamma)$ are also possible. These were judged unpromising in conventional WIMP models [41], but may be more interesting in the WIMPless models, where thermal relic constraints are effectively decoupled from observable signal strengths.

In addition, if the WIMPless explanation for the DAMA results holds, there are many striking implications for Higgs physics, which have been explored in detail in the related context of 4th generation quarks [40]. The Y connectors raise the Higgs boson mass far above the typical supersymmetric limit of 130 GeV, alleviating fine-tuning and making supersymmetry compatible with the golden Higgs signal region at the LHC. They also enhance $\sigma(gg \to h)$ by an order of magnitude, and strengthen the first-order electroweak phase transition, making electroweak baryogenesis viable [40]. Comprehensive detection strategies for this WIMPless model will have an interesting interplay with Higgs searches and other studies of new physics at the LHC.

7. Summary

One of the barriers to a theoretical understanding of the DAMA result is the difficulty in finding suitable candidates to explain it. In contrast to WIMPs, the WIMPless model proposed here easily matches the low mass and extremely high cross sections of the low mass DAMA region, while preserving the WIMP motivation of the naturally correct thermal relic density. This explanation implies specific and promising signals for other direct detection experiments and for indirect searches, such as GLAST, and the LHC. We note that the required DAMA cross sections are "extremely high" only when viewed from the WIMP viewpoint and are quite naturally achieved by the introduction of heavy colored fermions. This is a rather straightforward way to explain DAMA, and much of the discussion above will hold more generally in any model that explains DAMA in this way.

Acknowledgements

This work was supported by NSF grants PHY-0239817, PHY-0314712, PHY-0551164 and PHY-0653656, NASA grant NNG05-GG44G, and the Alfred P. Sloan Foundation. We are grateful to L. Bergstrom, D. Finkbeiner, P. Gondolo, M. Kaplinghat, G. Kribs, R. Mohapatra, S. Murgia, A. Pierce, H. Tu and H. Yu for discussions and thank the KITP, University of Michigan and University of New Mexico for hospitality.

References

[1] R. Bernabei, et al., arXiv: 0804.2741 [astro-ph].
[2] A.K. Drukier, K. Freese, D.N. Spergel, Phys. Rev. D 33 (1986) 3495;
K. Freese, J.A. Frieman, A. Gould, Phys. Rev. D 37 (1988) 3388.
[3] R. Bernabei, et al., Riv. Nuovo Cimento 26 (1) (2003) 1, astro-ph/0307403;
R. Bernabei, et al., Int. J. Mod. Phys. D 13 (2004) 2127, astro-ph/0501412.
[4] See, e.g., P. Belli, et al., Phys. Rev. D 61 (2000) 023512, hep-ph/9903501.
[5] J. Angle, et al., Phys. Rev. Lett. 100 (2008) 021303, arXiv: 0706.0039 [astro-ph].
[6] Z. Ahmed, et al., arXiv: 0802.3530 [astro-ph].
[7] P. Ullio, M. Kamionkowski, P. Vogel, JHEP 0107 (2001) 044, hep-ph/0010036;
A. Kurylov, M. Kamionkowski, Phys. Rev. D 69 (2004) 063503, hep-ph/0307185.
[8] R. Foot, arXiv: 0804.4518 [hep-ph].
[9] D.R. Smith, N. Weiner, Phys. Rev. D 64 (2001) 043502, hep-ph/0101138;
D.R. Smith, N. Weiner, Phys. Rev. D 72 (2005) 063509, hep-ph/0402065.
[10] P. Gondolo, G. Gelmini, Phys. Rev. D 71 (2005) 123520, hep-ph/0504010.
[11] R. Bernabei, et al., Eur. Phys. J. C 53 (2008) 205, arXiv: 0710.0288 [astro-ph].
[12] F. Petriello, K.M. Zurek, arXiv: 0806.3989 [hep-ph].
[13] A. Bottino, F. Donato, N. Fornengo, S. Scopel, arXiv: 0806.4099 [hep-ph].
[14] D. Stiff, L.M. Widrow, J. Frieman, Phys. Rev. D 64 (2001) 083516, astro-ph/0106048.
[15] J. Diemand, et al., arXiv: 0805.1244 [astro-ph].
[16] G. Angloher, et al., Astropart. Phys. 18 (2002) 43.
[17] D.S. Akerib, et al., Phys. Rev. Lett. 96 (2006) 011302, astro-ph/0509259.
[18] S.T. Lin, et al., arXiv: 0712.1645 [hep-ex].
[19] F.T. Avignone, P.S. Barbeau, J.I. Collar, arXiv: 0806.1341 [hep-ex].
[20] C.E. Aalseth, et al., arXiv: 0807.0879 [astro-ph].
[21] J. Abdallah, et al., Eur. Phys. J. C 31 (2004) 421, hep-ex/0311019.
[22] A. Bottino, F. Donato, N. Fornengo, S. Scopel, Phys. Rev. D 68 (2003) 043506, hep-ph/0304080;
A. Bottino, F. Donato, N. Fornengo, S. Scopel, Phys. Rev. D 77 (2008) 015002, arXiv: 0710.0553 [hep-ph].
[23] J.L. Feng, J. Kumar, arXiv: 0803.4196 [hep-ph].
[24] J.L. Feng, H. Tu, H.B. Yu, arXiv: 0808.2318 [hep-ph], JCAP, in press.
[25] M. Cvetič, G. Shiu, A.M. Uranga, Nucl. Phys. B 615 (2001) 3, hep-th/0107166.
[26] M.A. Shifman, A.I. Vainshtein, V.I. Zakharov, Phys. Lett. B 78 (1978) 443.
[27] J.R. Ellis, et al., Eur. Phys. J. C 24 (2002) 311, astro-ph/0110225.
[28] C. Boehm, P. Fayet, Nucl. Phys. B 683 (2004) 219, hep-ph/0305261.
[29] P.S. Barbeau, J.I. Collar, O. Tench, JCAP 0709 (2007) 009, nucl-ex/0701012.
[30] See, e.g., L. Bergstrom, P. Ullio, J.H. Buckley, Astropart. Phys. 9 (1998) 137, astro-ph/9712318.
[31] E.A. Baltz, J.E. Taylor, L.L. Wai, Astrophys. J. 659 (2007) L125, astro-ph/0610731.
[32] J.F. Navarro, C.S. Frenk, S.D.M. White, Astrophys. J. 462 (1996) 563, astro-ph/9508025.
[33] L.M. Widrow, J. Dubinski, Astrophys. J. 631 (2005) 838, astro-ph/0506177.
[34] S.D. Hunter, et al., Astrophys. J. 481 (1997) 205.
[35] L. Bergstrom, Phys. Lett. B 225 (1989) 372;
J.F. Beacom, N.F. Bell, G. Bertone, Phys. Rev. Lett. 94 (2005) 171301, astro-ph/0409403;
L. Bergstrom, T. Bringmann, M. Eriksson, M. Gustafsson, Phys. Rev. Lett. 95 (2005) 241301, hep-ph/0507229.
[36] L.E. Strigari, et al., Astrophys. J. 678 (2008) 614, arXiv: 0709.1510 [astro-ph].
[37] S. Rudaz, F.W. Stecker, Astrophys. J. 325 (1988) 16.
[38] I.V. Moskalenko, A.W. Strong, Phys. Rev. D 60 (1999) 063003, astro-ph/9905283.
[39] S.W. Barwick, et al., Astrophys. J. 482 (1997) L191;
M.A. DuVernois, et al., Astrophys. J. 559 (2001) 296.
[40] G.D. Kribs, T. Plehn, M. Spannowsky, T.M.P. Tait, Phys. Rev. D 76 (2007) 075016, arXiv: 0706.3718 [hep-ph];
R. Fok, G.D. Kribs, arXiv: 0803.4207 [hep-ph].
[41] A. Birkedal, K. Matchev, M. Perelstein, Phys. Rev. D 70 (2004) 077701, hep-ph/0403004;
J.L. Feng, S. Su, F. Takayama, Phys. Rev. Lett. 96 (2006) 151802, hep-ph/0503117.